INTERNATIONAL JOURNAL OF AGRICULTURE & BIOLOGY
ISSN Print: 1560–8530; ISSN Online: 1814–9596
12–267/2012/14–5–689–696
http://www.fspublishers.org

Full Length Article

Evaluating and Classifying Field-Scale Soil Nutrient Status in Beijing using 3S Technology

JIN-LING ZHAO, YONG-AN XUE[1]†, HAO YANG, LIN-SHENG HUANG‡ AND DONG-YAN ZHANG‡
Beijing Research Center for Information Technology in Agriculture, Beijing 100097, China
†College of Mining Engineering, *Taiyuan University of Technology, Taiyuan 030024, China*
‡*Key Laboratory of Intelligent Computing & Signal Processing, Ministry of Education, Anhui University, China*
[1]Corresponding author's e-mail: anantyut@163.com

ABSTRACT

More attention has been paid to estimating soil nutrient status, along with a sharp decrease in total farmland acreage, especially in Beijing Municipality. However, traditional site-specific investigation makes it impossible to apply it to large scale monitoring. The objective of this study was to evaluate and classify soil nutrient status using advanced 3S (global positioning system, GPS; remote sensing, RS; and geographic information system, GIS) technology. Firstly, multi-temporal Landsat TM 5 images with 30 m spatial resolution were utilized to identify the field-scale farmlands. The overall classification accuracy reached 86.96%, with a *kappa* coefficient of 0.743. Additionally, the correlation coefficient (*r*) reached 0.942 by comparing the remote sensing-based farmland area with the statistical data. Subsequently, organic matter, total nitrogen, available phosphorus and available potassium from 7,435 field sample points positioned by GPS receiver, were used to generate a comprehensive soil nutrient index in GIS software, according to the classification criteria of Beijing Soil and Fertilizer Workshop. Finally, a classification map of field-scale soil nutrient levels (very high, high, moderate, low & very low) was created using the farmlands as mask layers. The analysis results showed that the soils at moderate and low levels dominated the Beijing's farmlands, which accounted for 46.1% and 39.1%, respectively; high and very low level soils were the second place whose ratios were 10.4% and 4.3%, respectively; and very high level soils could be rarely found. Yanqing County, Tongzhou District and Changping District have better soil nutrient status as a whole.

Key Words: Beijing city; Geospatial analysis; Remote sensing; Soil nutrient status assessment; Spatial interpolation

INTRODUCTION

Farmland, as one of our most basic natural resources, has provided the basic production materials for human beings to ensure crop safety. However, with the rapid development of society and economy as well as the increasing population growth, the total quantity of farmland has been decreasing. As a developing country, China with vast population and scarce land per capita has been experiencing a rapid expansion from farmland to industrial and residential uses (Tan *et al*., 2005). Consequently, the conflict between humans and farmlands has been greatly sharpened, especially in the regions with a well-developed economy (Yang & Li, 2000). To cherish and rationally utilize farmland resources, a number of measures have been carried out in China in order to achieve sustainable development of agriculture. The Chinese government has made farmland protection as a national strategic issue in ensuring sustainable socio-economic development, which must be strictly implemented for a long term (Lichtenber & Ding, 2008). Given recent trends of decreasing farmland quantity, a number of studies have been performed on how to assess and improve the farmland quality (McClaran *et al*., 1985; Parr *et al*., 1992; Parks & Quimio, 1996; Gui *et al*., 2009). On the basis of ensuring the quantity of farmland, how to improve the farmland quality has been considered to be a hot spot until recently. Among the various affecting factors to determine farmland quality, soil fertility is one of the important factors, which has an important economic value for the fast-growing economic regions, but it is environmentally unstable (Wander *et al*., 2002; Qi *et al*., 2009; Hussain *et al*., 2010; Jabbar *et al*., 2011).

Traditionally, the farmland information monitoring mainly depend on manually collecting site-specific data in the field by technical person. Conversely, innovative earth observation techniques, especially the remote sensing (RS) technology, have been extensively applied in corresponding studies on cropland landscape, arable land loss, spatial and temporal patterns of farmland, etc. (Xiao *et al*., 2002; Liu *et al*., 2005; Tan *et al*., 2005). However, most previous studies have primarily focused on the identification of farmland, farmland mapping and land use and land cover change (LUCC) using remote sensing dataset (Ramankutty & Foley, 1999; Wen, 2002; Xiao *et al*., 2006). Recently, the studies on farmland have transferred from quantity monitoring to the focus on the parallel analysis of quantity,

To cite this paper: Zhao, J.L., Y.A. Xue, H. Yang, L.S. Huang and D.Y. Zhang, 2012. Evaluating and classifying field-scale soil nutrient status in Beijing using 3S technology. *Int. J. Agric. Biol*., 14: 689–696

quality and ecological benefits. Nevertheless, remote sensing techniques have not been integrated into the assessment of soil nutrient status.

As one of the fastest growing economic municipalities along with rapid urban sprawl in China, Beijing's land use structures have been greatly changed since the 1980s. The most obvious feature is that the total amount of farmland has been decreasing. In comparison with the area of 4,560 km^2 at the initial stage of reforming and opening up in 1981, the farmland area has decreased to 2,876 km^2 in 2001; while the number of population has increased to 17,550 thousand in 2009 from 8,715 thousand in 1978 (Beijing Statistical Information Net, http://www.bjstats.gov.cn/). Additionally, the farmland in Beijing has also been confronting the threats of quality decreasing, salinization, soil pollution, etc. Consequently, based on identifying farmlands, estimating and classifying the field-scale soil nutrient status is of great importance for mastering regional farmland resources and managing production practices, especially for the soil testing and fertilization (Pathak *et al*., 2003). Concerning the soil nutrient status of Beijing, some studies have been performed. Kong *et al*. (2003), based on the soil sample data acquired using a global positioning system (GPS) receiver, explored the change features and spatial distribution of soil nutrient of the urban-rural ecotone in Daxing District using spatial analysis techniques and Kriging interpolation method in geographic information system (GIS) software. Su *et al*. (2000) analyzed the soil fertility of farmlands in Haidian District and the result showed that it was generally at a moderate level. Lu *et al*. (2005) investigated the distribution and change features of farmland soil quality in Pinggu District, which showed that the soil nutrient status was generally at a moderate level.

The above literature clearly shows that two limitations in investigating the soil nutrient status in Beijing could be found from previous studies. One is that the spatial scales of the study sites were comparatively small, because most of studies focused on a certain district or smaller region. The other is that statistical analysis methods based on sampling point data, were mainly used in traditional soil nutrient monitoring, and conversely, field-scale studies have not been fully carried out. The aims of the study were to (1) identify field-scale farmlands of Beijing using multi-temporal Landsat TM 5 images; (2) explore and classify the field-scale soil nutrient status by spatial analysis and geostatistical functions in GIS software; and (3) analyze the spatial distribution characteristics of farmlands and corresponding soils with different nutrient levels.

MATERIALS AND METHODS

Introduction to the study site: Beijing, as the capital city of the People's Republic of China, is located in the northern part of North China Plain, with a longitude range between 115°25'-117°20' East and a latitude range between 39°38'-40°51' North (Fig. 1a). Its geomorphological types consist of the northwestern mountains and southeastern plains and the general terrain is high in the northwest and low in the southeast. In the plain areas, the elevations are generally between 20 and 60 m in most regions (Fig. 1b). Conversely, they are located between 1,000 and 1,500 m in the mountain regions. Beijing has a sub-humid warm temperature climate zone, with an annual average rainfall of 430.9 mm, an annual average temperature of 13.1°C and a frost-free period of 185 days. The coldest month is January and the average temperature throughout the whole year is -3.9°C, while the average temperature of the hottest month (July) is 26.5°C. According to the statistical data from Beijing Municipal Bureau of Land and Resources, there is totally 16,410 km^2 land area, among which the area of plains is 6,338 km^2 (38.6%) and it is 10,072 km^2 (61.4%) for the mountains. By the end of 2010, Beijing was administratively divided into fourteen districts and two counties in accordance with the Beijing Statistical Yearbook 2010. In those administrative divisions, Mentougou District, Huairou District, Pinggu District, Miyun County and Yanqing County were specified as the ecological conservation areas and they are also the regions with most croplands at the same time. In 2008, there was totally 10,959.81 km^2 cropland and the farmland area was 2,316.88 km^2. Yanqing County, Huairou District and Miyun County were the top three regions, which had the most farmlands. Wheat, maize and vegetation are the major crops in Beijing and their planting area were 226,000 ha, 151,000 ha and 68,000 ha, respectively, in 2009.

Data sources and preprocessing: Two types of dataset including remotely sensed images and soil sampling field data were required in this study. Multi-temporal Landsat TM 5 images were selected in our study. This satellite has a spatial resolution in 30 m, a swath width in 185 km and a 16d revisiting period, which includes six multispectral bands with a spectral range of 0.45-2.35 μm and a thermal infrared band, with a spatial resolution of 120 m and a spectral range of 10.40-12.50 μm. Two scenes, with the paths and rows of p123/r32 and p123/r33, were required to cover the whole study area. To accurately identify the spatial distribution of field-scale farmlands, multi-temporal images were acquired during the growing seasons of various grain crops. Three images (15 April, 20 July and 22 September) of p123/r32 were totally acquired in 2009 and only an image of p123/r33 was collected due to its small percentage of covering the study area. Before identifying farmland fields using the remote sensing images, some preprocessing procedures must be firstly performed including radiometric calibration, atmospheric correction and geometric correction. In our study, radiometric calibrations were conducted in accordance with the header information from Landsat TM 5 images in ENVI (The Environment for Visualizing Images, Research Systems, Inc.) image analysis software, and then atmospheric corrections were carried out using the FLAASH (Fast Light-of-sight Atmospheric

Analysis of Spectral Hypercubes) module integrated with ENVI. Subsequently, geometric corrections including plane corrections and ortho-rectifications were conducted in ERDAS (Earth Resource Data Analysis System) image processing system, which required that the root mean square errors (RMSEs) were within 0.5 pixels. The reference images for geometric corrections were taken from the Landsat Geocover dataset (http://glcf.umiacs.umd.edu/), which provided a collection of high resolution satellite imagery in a standardized, orthorectified format, and the ASTER (Advanced Thermal & Emission Radiometer) GDEM (Global Digital Elevation Map) images from https://wist.echo.nasa.gov/api/ with 30 m spatial resolution were used as the elevation reference images. After the images were preprocessed, image mosaicing of two scenes and masking by the Beijing administrative boundary were performed to generate the remote sensing image of Beijing Municipality.

The site-specific soil nutrient data were the 7,435 field sampling points collected in 2008 and they were positioned using a sub-meter GPS receiver (Fig. 1b). Table I was the collected soil nutrient indicators for each sampling point. Afterwards, those point data with longitude and latitude coordinates were imported into ArcMap platform and were further converted into ESRI shapefile format for subsequent geospatial analysis and interpolation. Finally, they were statistically preprocessed including frequency analysis, central tendency, degree of dispersion and distribution characteristics in ArcMap, and were interpolated to map the soil nutrient indicators.

Identification of field-scale farmlands using remotely sensed images: Multi-temporal Landsat TM 5 images were used to identify field-scale farmlands by support vector machine (SVM) supervised classification in ENVI (Lv & Liu, 2010). Water body, vegetation and non-vegetation areas were only selected as the regions of interest (ROIs) to perform classification, and three classification maps were obtained. Then, those maps were layerstacked to form a merged map according to the acquisition time, and the classification was further performed on the layerstacked map by selecting specific ROIs. When water bodies, forest lands and built-up areas were removed from the classification results, the farmland map was obtained and converted to shapefile format after post-classification processes including seiving classes, combine classes, etc. To validate the identification result, two methods were utilized simultaneously: one was to form a confusion matrix to calculate the overall classification accuracy and *kappa* coefficient; and the other was to evaluate the classification accuracy by the farmland statistical area from Beijing statistical information net (BSIN, http://www.bjstats.gov.cn/sjfb/bssj/ndsj/).

$$Kappa = \frac{N\sum_{i=1}^{k} x_{ii} - \sum_{i=1}^{k} x_{i\Sigma} x_{\Sigma i}}{N^2 - \sum_{i=1}^{k} x_{i\Sigma} x_{\Sigma i}} \qquad (1)$$

Where, N is the total number of pixels in all the ground truth classes; x_{ii} is the confusion matrix diagonals; k is the total classes; $x_{i\Sigma}$ is the sum of the ground truth pixels in i class; $x_{\Sigma i}$ is the sum of the classified pixels in that class.

Classification criteria for soil nutrient status: The classification criteria adopted hear was the regulation for gradation and classification on soil nutrient developed by Beijing Soil and Fertilizer Work Station (BSFWS) in December 2006. In this regulation, four indicators including organic matter, total nitrogen (N) or alkali-hydrolyzable N, available phosphorus (P) and available potassium (K) were selected. At the same time, referring to the historical documents and experts' suggestions, the weighted coefficients and scores of each indicator were also given according to the soil nutrient features and the contributions to soil nutrient status (Table Π). In addition, a comprehensive index called the soil nutrient index (SNI) was also recommended by the BSWFS, which was calculated by the weighted-sum method (Eq. 2).

$$SNI = \sum F_i \times W_i \quad (i=1, 2, 3, ..., n) \qquad (2)$$

Where Fi is the score value of the ith edaphic indicator; Wi is the weighted coefficient of the ith edaphic indicator; n is the total number of selected edaphic indicators.

Spatial interpolation of soil nutrient indicators: To perform the rater calculation in ArcGIS Spatial Analyst, those sampling point data of soil nutrient must be interpolated to rater format. An interpolation method must be used for generating continuous surface grids from point data. Three types of interpolation methods including inverse distance weighted (IDW), Spline and Kriging are available in ArcMap platform. Considering the distribution of large amount of sample points, Kriging was utilized in our study and the Kriging estimator is given by a linear combination (Eq. 3). This method is a group of geostatistical techniques to interpolate the value of a random field at an unobserved location from observations of its value at nearby locations (Oliver & Webster, 1990). It has been widely applied in diverse research fields such as underground water simulation, soil mapping (Hengl *et al*., 2004; Rabelo & Wendland, 2009). Consequently, four raster interpolation maps with 30 m spatial resolution of four soil indicators were created using such a method. Then, the SNI was calculated using the raster calculator tool in ArcMap according to the Eq. 2 and Table Π. Finally, the level classification map of soil nutrient status was generated and exported to raster format with 30 m using the SNI values of each pixel. When the map was masked by the Beijing administrative boundary and field-scale farmland map, the soil nutrient levels of Beijing were specified.

$$\hat{Z}(x_0) = \sum_{i=1}^{n} \omega_i(x_0) Z(x_i) \qquad (3)$$

Where $Z(x_0)$ represents the value of a random field $Z(x)$ at an unobserved location x_0; $\hat{Z}(x_0)$ is the best linear unbiased estimator of $Z(x_0)$; $Z(x_i)$ are the observed values, i=1, 2, …, n of the random field at nearby locations; and ω_i are the weights, i=1, 2, …, n.

RESULTS

Identified farmlands and their spatial distribution: It could be found that the land features in bright purple color were generally classified as the farmlands by comparing the original false color fused image (Fig. 2a) and the identified farmlands (Fig. 2b). After obtaining the farmlands based on remotely sensed images, it was extremely necessary to validate its classification for subsequent analysis. According to the confusion matrix, the overall classification accuracy reached 86.96%, with a *kappa* coefficient of 0.743. In addition, the linear regression was performed between the remote sensing-based farmland area and the statistical data from the BSIN. The correlation coefficient (r) reached 0.942 (Fig. 3). In the identified result (Fig. 2b), farmlands in Beijing mainly distributed in the southeastern plain areas. Specifically, the farmland distributions in Tongzhou District, Shunyi District, and Daxing District were the densest, which covered most of the land cover types in three districts. Conversely, due to the existence of mountain geomorphology, most of farmlands distributed just in the plain regions in Fangshan District, Mentougou District, Huirou District, Pinggu District, Changping District, Miyun County and Yanqing County. In the central regions of Beijing, built-up areas dominates the land use types and there was nearly no farmlands in Chaoyang District, Shijingshan District, Fengtai District and central urban areas.

Descriptive statistics of soil nutrient indicators: Depending on the interpolated raster maps of four soil indicators, descriptive statistics were performed by Beijing's administrative divisions (Table III). For the organic matter, it had the highest content in Fangshan District and the mean was 23.34 g kg^{-1}, while it had also the maximum standard deviation (StdDev) of 23.69, which showed that the spatial dispersion of this indicator was the largest in this region. Conversely, Pinggu District had the lowest content and its mean was only 1.78 g kg^{-1}, and its StdDev (0.77) was also the smallest. Considering the total N, Huairou District had

Table I: Indicators description of several sampling points of soil nutrient

No.	Land use type	Organic matter (g kg^{-1})	Available P (mg kg^{-1})	Available K (mg kg^{-1})	Total N (g kg^{-1})	Soil PH	Alkali-hydrolyzable N (mg kg^{-1})	Slowly available K (mg kg^{-1})
1	Summer maize	17.38	20.17	96.00	0.92	8.49	61.00	796.00
2	Winter wheat	17.28	10.34	90.00	0.97	8.28	79.00	706.00
3	Spring maize	13.36	30.79	82.00	0.85	8.12	65.00	582.00
4	Summer maize	18.55	15.45	108.00	1.15	8.13	138.00	592.00
5	Spring maize	19.28	85.25	160.00	1.21	7.93	97.00	528.00
6	-	10.24	4.44	64.00	0.73	8.39	52.00	432.00
7	-	11.09	12.50	80.00	0.66	8.65	51.00	596.00
…	…	…	…	…	…	…	…	…

Table II: Scores and weighted coefficients of selected edaphic indicators to classify the soil nutrients*

Level	Organic matter (g kg^{-1})/score	Total N (g kg^{-1})/score	alkali-hydrolyzable N (g kg^{-1})/score	Available P (g kg^{-1})/score	Available K (g kg^{-1})/score	SNI
Very high	≥25/100	≥1.20/100	≥120/100	≥90/100	≥155/100	100-95
High	(25-20)/80	(1.20-1.00)/80	(100-90)/80	(90-60)/80	(155-125)/80	95-75
Moderate	(20-15)/60	(1.00-0.80)/60	(90-60)/60	(60-30)/60	(125-100)/60	75-50
Low	(15-10)/40	(0.80-0.65)/40	(60-45)/40	(30-15)/40	(100-70)/40	50-30
Very low	<10/20	<0.65/20	<45/20	<15/20	<70/20	30-0
Weight	0.3	0.25		0.25	0.20	-

*Data source: http://nw.bjtzh.gov.cn/tongzhouweb/new%20soil/trfl-yfpj-pingjiafangfa.html.

Table III: Descriptive statistics of soil nutrient indicators according to Beijing's administrative divisions

Region	No.	Organic matter (g kg^{-1})				Total N (g kg^{-1})				Available P (g kg^{-1})				Available K (g kg^{-1})			
		Max	Min	Mean	SD	Max	Min	Mean	SD	Max	Min	Mean	SD	Max	Min	Mean	SD
Huairou	13	28.82	10.55	17.01	4.86	1.87	0.64	1.04	0.32	185.61	5.52	50.08	53.07	302.40	73.32	153.69	63.60
Miyun	502	67.00	0.85	14.74	6.64	0	3.41	0.84	0.37	401.7	1.93	23.26	32.04	700.00	4.93	144.80	77.89
Changping	766	56.52	1.41	17.13	6.17	3.17	0.13	0.98	0.33	204.84	1.21	35.53	40.29	948.73	17.48	135.61	130.50
Shunyi	375	28.63	5.53	15.14	3.53	2.32	0.38	0.94	0.26	286.21	1.29	30.47	35.79	948.00	44.00	114.62	77.98
Pinggu	1174	5.51	-0.14	1.78	0.77	0.26	0	0.11	0.03	350.60	0	32.58	37.38	1180.00	0	185.85	132.05
Tongzhou	1466	38.9	1.26	16.95	4.56	5.88	0.07	0.98	0.34	544.4	0.3	48.00	55.55	950.0	40.0	160.67	90.19
Daxing	413	26.11	2.45	11.78	4.10	1.39	0	0.18	0.34	351.5	1.1	29.77	39.40	1206.1	21.1	110.03	109.21
Fangshan	1788	435.42	0.08	23.34	23.69	-	-	-	-	884.75	0.24	34.72	47.38	3330.05	0	176.49	167.60
Mentougou	778	8.75	0.06	2.37	1.15	3.75	0	0.71	0.43	316.33	0.02	17.23	27.13	950.00	0	204.00	138.10
Beijing	**7275**	**435.42**	**-0.14**	**13.99**	**14.49**	**5.88**	**0**	**0.52**	**0.51**	**884.75**	**0**	**33.53**	**44.01**	3330.05	0	**162.92**	**130.67**

the highest content and its mean was 1.04 g kg^{-1}, while it was lowest in Pinggu District with only a mean of 0.11 g kg^{-1}. In addition, Huairou, Miyun, Changping, Shunyi, Tongzhou and Daxing had the similar StdDev (near 0.3) in total N, which showed that those regions had the very similar dispersion in this indicator. Conversely, Pinggu had the smallest dispersion with only a StdDev of 0.03. In the available P, Huairou had the highest content and the mean was 50.08 g kg^{-1}, while Mentougou had the smallest content with only a mean of 17.23 g kg^{-1}. The StdDev of this indicator was maximum (55.55) in Tongzhou and minimum (27.13) in Mentougou. In the available K, Huairou had also the highest content and the mean was 204.00 g kg^{-1}, while Daxing had the smallest content with only a mean of 17.23 g kg^{-1}. The StdDev of this indicator was maximum (167.60) in Fangshan and minimum (63.60) in Huairou. As a whole, in four soil nutrient indicators, the StdDev of available K was the largest which showed that this indicator had the largest differences in different regions. Conversely, the total N had the smallest changes among those administrative divisions.

Assessment of soil nutrient levels: As shown in the soil nutrient level map (Fig. 4a), we could find that the overall soil nutrient status was low in Beijing. After statistically and spatially investigating the classification result, the analysis results showed that the soil nutrient status in Beijing was generally at moderate and low levels, which accounted for 46.1% and 39.1%, respectively. The moderate level soils primarily distributed in Yanqing, Tongzhou, Fangshan and Shunyi, while the low level soils could be found in Daxing, Miyun and Pinggu. In comparison with the moderate and low level soils, their ratios were 10.4% and 4.3%, respectively for the soils at high and very low levels. The high level soils primarily distributed in Yanqing, Tongzhou, Changping, Haidian and Shunyi, while they could be found in Daxing, Miyun and Pinggu for the very low level soils. Conversely, there were almost no very high level soils. To validate the classification accuracy, the monitoring results from the BSFWS were used, which were obtained by 292 long-term monitoring points at fixed sites. According to the monitoring report from the BSFWS in 2006, the ratio of soils with very high, high, moderate, low and very low levels were 0.7%, 17.5%, 44.4%, 34.3% and 3.1% in comparison with 0%, 10.4%, 46.1%, 39.1% and 4.3% derived from 3S technology.

DISCUSSION

As can be seen in Fig. 2a, different land features have very diverse colors and textures in the false color fused

Fig. 1: Geographic location (a) and elevation (b) maps of the study site

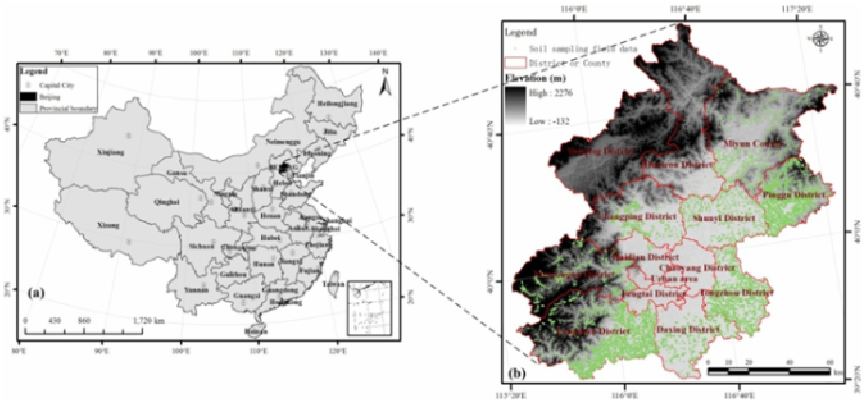

Fig. 2: The identified farmland fields of Beijing City using multi-temporal Landsat TM 5 remotely sensed images

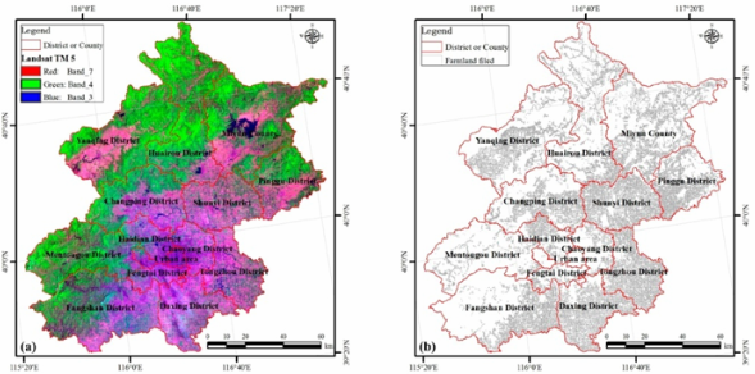

image. However, confusion class phenomena still exited among different land features such as farmlands and built-up areas. Specifically, a farmland show in light purple, while a built-up area shows in deep purple. Therefore, to more accurately identify the farmlands, more comprehensive information must be used to better separate the farmlands from other land features including spectra, texture, digital elevation model (DEM) as well as its derived slope and aspect, etc. Additionally, the seasonal characteristics of green vegetation must also be considered. In comparison with single image, multi-temporal images have more seasonal features for identifying specific land features, especially for those objects covered with grain crops (Maracci & Aifadopoulou, 1990; Murthy *et al*., 2003). Phenology information is a useful addition in assisting in selecting the optimal remotely sensed images (Vina *et al*., 2004; Richardson *et al*., 2009). After obtaining the field-scale farmlands, its classification accuracy must be validated to determine whether it could meet the accuracy requirement for further spatial analysis of soil nutrient status (Lucas *et al*., 1994; Congalton & Green, 1999).

However, according to the distribution trend of data point in Fig. 3, the farmland area derived from remote sensing images was generally greater than that from statistical data for most of districts and counties. The reason for this phenomenon was that they mainly considered the land use properties and categorized those land features used to plant grain crops as the farmlands for the statistical data. Conversely, in the process of identifying farmlands using remote sensing images, the land features were classified as farmlands in accordance with the spatial structure, texture and spectral information from selected ROIs. As a result, unused land, bare land and some built-up areas were wrongly classified as farmlands, so the area was greater than that of statistical data. Due to the constraint of spatial and spectral resolutions for Landsat TM images, mixed pixels and spectral similarities caused the misclassification and omission in identifying farmlands. To obtain more detailed farmland information, remotely sensed images with higher

Fig. 3: Comparative analysis between remote sensing based farmlands area and statistical data

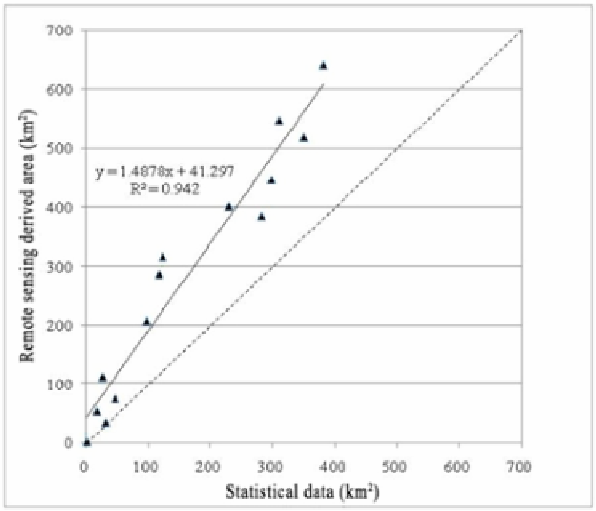

spatial resolutions have to be acquired such as QuickBird, SPOT, IKONOS (Yang *et al*., 2007; Levinab *et al*., 2009; Zhang *et al*., 2010).

The levels of soil nutrient status were further classified on the basis of identifying field-scale farmlands. After classifying the soil nutrient levels, it was extremely necessary to verify the classification accuracy. In this study, statistical data were used to compare with the identification result derived from 3S technology. Specifically, the moderate level soils were taken as an example to compare the classification with statistical data (Fig. 4b). It could be found that there were some differences between remote sensing derived and statistical data. Especially, the difference was the largest in Pinggu District, because the farmlands there were primarily used to plant fruit trees and they were mainly used for planting grain crops in other districts or counties. The comparative analysis showed that there were some differences between the assessment result in this study and the monitoring result from the BSFWS. The reason was that the monitoring result from the BSFWS

Fig. 4: Spatial distribution of field-scale soil nutrient levels of Beijing City

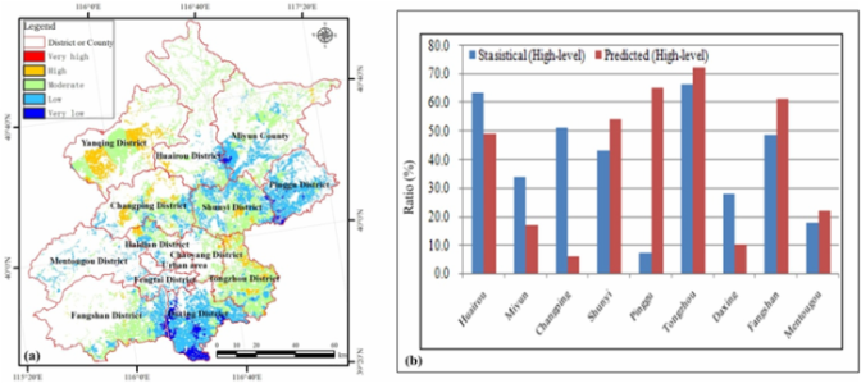

was obtained by statistical analysis, while remote sensing derived classification considered all the farmlands. Another reason is that specific geomorphic types have also determined that the spatial distribution of farmlands is not even in the study site, so the field sample point layout cannot cover the whole study area. Consequently, the number of sample data is larger in the regions with dense farmlands, while it is small or none in the mountain areas. The spatial interpolation accuracies of four edaphic indicators will be affected to a certain degree. In addition, only four soil indicators (organic matter, total N, available P & available K) were incorporated into the assessment index in our study, so it is inevitable that the comprehensive integrity of SNI is not very satisfactory. More indicators will be considered in the subsequent analysis. Furthermore, some soil nutrient indicators usually show the variable characteristics due to the influence of human activities, multi-temporal assessments of soil nutrient status will be required to reflect the dynamic change process over a certain times pan. In the further research, to better improve the soil quality, it is more essential to find out the primary driving factors, which cause the changes of soil nutrient status and provide effective strategies by analyzing time series soil nutrient conditions (Wang & Gong, 1998; Arshad & Martin, 2002; Chen *et al.*, 2006).

In conclusion, advanced 3S technology can fast and effectively identify field-scale farmlands and map the soil nutrient status over a large spatial scale, but more field sampling data must be required as the prior knowledge to assist in classification and validation. It is required that multi-temporal remotely sensed images are used to identify farmlands due to the bad influence of similarities between different land features. The Landsat TM 5 images with 30 m spatial resolution can satisfy the needs of identifying farmlands and classifying field-scale soil nutrient status. However, there are some differences between the statistical and remote sensing derived data, due to their different analysis principles. To better validate the classification accuracy derived from Landsat TM images, the images with more high spatial resolution will be needed in future studies.

Acknowledgement: This work was supported by Beijing Postdoctoral Research Foundation (2012), Postdoctoral Science Foundation of Beijing Academy of Agriculture and Forestry Sciences (2011) and the National Science and Technology Support Program' the Technology of Remote Sensing Monitoring Key Indicators of Cultivated Land Quality'(2012BAH29B01).

REFERENCES

Arshad, M.A. and S. Martin, 2002. Identifying critical limits for soil quality indicators in agro-ecosystems. *Agric. Ecosyst. Environ*., 88: 153–160

Chen, J., Z.R. Yu, J. Ouyang and M.E.F. Van Mensvoort, 2006. Factors affecting soil quality changes in the North China Plain: A case study of Quzhou County. *Agric. Syst.*, 91: 171–188

Congalton, R.G. and K. Green, 1999. *Assessing the Accuracy of Remotely Sensed Data: Principle and Practices,* 2nd edition. Lewis Publishers, New York, USA

Gui, D.W., J.Q. Lei, G.J. Mu and F.J. Zeng, 2009. Effects of different management intensities on soil quality of farmland during oasis development in southern Tarim Basin, Xinjiang, China. *Int. J. Sustain. Dev. World*, 16: 295–301

Hengl, T., G.B.M. Heuvelink and A. Stein, 2004. A generic framework for spatial prediction of soil variables based on regression-kriging. *Geoderma*, 120: 75–93

Hussain, A., G. Murtaza, A. Ghafoor, S.M.A. Basra, M. Qadir and M. Sabir, 2010. Cadmium contamination of soils and crops by long term use of raw effluent, ground and canal waters in agricultural lands. *Int. J. Agric. Biol.*, 12: 851–856

Jabbar, A., R. Ahmad, I.H. Bhatti, T. Aziz, M. Nadeem, W.U. Din and A.U. Rehman, 2011. Residual soil fertility as influenced by diverse rice-based inter/relay cropping systems. *Int. J. Agric. Biol*., 13: 477–483

Kong, X.B., F.R. Zhang, R. Wang and Y. Xu, 2003. GIS based analysis of spatial-temporal distribution of soil nutrients in a suburb region: A case study of the Daxing district in Beijing City. *Acta Ecol. Sin.*, 23: 2210–2218

Levinab, N., C. McAlpineb, S. Phinnb, B. Priceb, D. Pullarb, R.P. Kavanaghc and B.S. Lawc, 2009. Mapping forest patches and scattered trees from SPOT images and testing their ecological importance for woodland birds in a fragmented agricultural landscape. *Int. J. Remote Sens*., 30: 3147–3169

Lichtenber, E. and C.R. Ding, 2008. Assessing farmland protection policy in China. *Land Use Policy*, 28: 59–68

Liu, J.Y., M.L. Liu, H.Q. Tian, D.F. Zhuang, Z.X. Zhang, W. Zhang, X.M. Tang and X.Z. Deng, 2005. Spatial and temporal patterns of China's cropland during 1990-2000: An analysis based on Landsat TM data. *Remote Sens. Environ.*, 98: 442–456

Lu, P., S.Y. Wang, J.L. Wang, L. Yang, K. Yang, Z.G. Zhang and T.Q. Yu, 2007. Review and change of arable soil nutrients content in Pinggu District of Beijing. *Beijing Agric.*, 33: 28–34

Lucas, I.F.J., J.M. Frans and V.D. Wel, 1994. Accuracy assessment of satellite derived land-cover data: A review. *Photogramm. Eng. Rem. S.*, 60: 410–432

Lv, T.T. and C. Liu, 2010. Study on extraction of crop information using time-series MODIS data in the Chao Phraya Basin of Thailand. *Adv. Space Res*., 45: 775–784

Maracci, G. and D. Aifadopoulou, 1990. Multi-temporal remote sensing study of spectral signatures of crops in the Thessaloniki test site. *Int. J. Remote Sens*., 11: 1609–1615

McClaran, M.P., J. Romm and J.W. Bartolome, 1985. Differential farmland assessment and land use planning relationships in Tulare County, California. *J. Soil Water Conserv*., 40: 252–255

Murthy, C.S., P.V. Raju and K.V.S. Badrinath, 2003. Classification of wheat crop with multi-temporal images: performance of maximum likelihood and artificial neural networks. *Int. J. Remote Sens.*, 24: 4871–4890

Oliver, M.A. and R. Webster, 1990. "Kriging: a method of interpolation for geographical information system". *Int. J. Geogr. Inf. Syst.*, 4: 313–332

Parks, P.J. and W.R.H. Quimio, 1996. Preserving agricultural land with farmland assessment: New Jersey as a case study. *Agric. Resou. Econ. Rev*., 25: 22–27

Parr, J.F., R.I. Papendick, S.B. Hornick and R.E. Meyer, 1992. Soil quality: Attributes and relationship to alternative and sustainable agriculture. *American J. Altern. Agric*., 7: 5–11

Pathak, H., P.K. Aggarwal, R. Roetter, N. Kalra, S.K. Bandyopadhaya, S. Prasad and H. Van Keulen, 2003. Modelling the quantitative evaluation of soil nutrient supply, nutrient use efficiency, and fertilizer requirements of wheat in India. *Nutr. Cycl. Agroecosyst.*, 65: 105–133

Qi, Y.B., J.L. Darilek, B. Huang, Y.C. Zhao, W.X. Sun and Z.Q. Gu, 2009. Evaluating soil quality indices in an agricultural region of Jiangsu Province, China. *Geoderma*, 149: 325–334

Rabelo, J.L. and E. Wendland, 2009. Assessment of groundwater recharge and water fluxes of the Guarani Aquifer System, Brazil. *Hydrogeol. J.*, 17: 1733–1748

Ramankutty, N. and J.A. Foley, 1999. Estimating historical changes in global land cover: Croplands from 1700 to 1992. *Global Biogeochem. Cycl.*, 13: 997–1027

Richardson, A.D., B.H. Braswell, D.Y. Hollinger, J.P. Jenkins and S.V. Ollinger, 2009. Near-surface remote sensing of spatial and temporal variation in canopy phenology. *Ecol. Appl.*, 19: 1417–1428

Su, L.X., S.Q. Wang, J. Xiao and X. Wang, 2005. Study on the nutrients of arable soil in Haidian District of Beijing. *J. Beijing Agric. Coll.*, 20: 53–57

Tan, M.H., X.B. Li, H. Xie and C.H. Lu, 2005. Urban land expansion and arable land loss in China-a case study of Beijing-Tianjin-Hebei region. *Land Use Pol.*, 22: 187–196

Vina, A., A.A. Gitelson, D.C. Rundquist, G. Keydan, B. Leavitt and J. Schepers, 2004. Monitoring maize (*Zea mays* L.) phenology with remote sensing. *Agron. J.*, 96: 1139–1147

Wander, M.M., G.L. Walter, T.M. Nissen, G.A. Billero, S.S. Andrews and D.A. Cavanaugh-Grant, 2002. Soil quality: science and process. *Agron. J.*, 94: 23–32

Wang, X.J. and Z.T. Gong, 1998. Assessment and analysis of soil quality changes after eleven years of reclamation in subtropical China. *Geoderma*, 81: 339–355

Wen, Q.H., 2002. Land use change analysis in the Zhujiang Delta of China using satellite remote sensing, GIS and stochastic modeling. *J. Environ. Manage*., 64: 273–284

Xiao, J.Y., Y.J. Shen, J.F. Ge, R. Tateishi, C. Tang, Y.Q. Liang and Z.Y. Huang, 2006. Evaluating urban expansion and land use change in Shijiazhuang, China, by using GIS and remote sensing. *Landscape Urban Plan*., 75: 69–80

Xiao, X., S. Boles, S. Frolking, W. Salas, B. Moore III, C. Li, L. He and R. Zhao, 2002. Landscape-scale characterization of cropland in China using Vegetation and Landsat TM images. *Int. J. Remote Sens*., 23: 3579–3594

Yang, C.H., J.H. Everitt, R.S. Fletcher and D. Murden, 2007. Using high resolution QuickBird imagery for crop identification and area estimation. *Geocarto Int.*, 22: 219–233

Yang, H. and X.B. Li, 2000. Cultivated land and food supply in China. *Land Use Pol.*, 17: 73–88

Zhang, X.Y., X.Z. Feng and H. Jiang, 2010. Object-oriented method for urban vegetation mapping using IKONOS imagery. *Int. J. Remote Sens*., 31: 177–196

(Received 30 May 2012; Accepted 18 July 2012)